Roll-to-Roll Fabrication of PEDOT:PSS Stripes Using Slot-Die Head With μ-Tips for AMOLEDs

Gieun Kim, Jinyoung Lee, Dong-Kyun Shin, and Jongwoon Park

***Abstract*— Stripe coating offers an approach to remove the pixel bank structure used to confine ink droplets. For potential application in solution-processable active-matrix organic light-emitting diode displays, we fabricate fine and dense stripes of poly(3,4-ethylenedioxythiophene): poly(4-styrenesulfonate) (PEDOT:PSS) using a slot-die head with the dual plate (shim plate with slit channels and meniscus-guiding plate with μ-tips as narrow as pixels). We analyze the flow distribution of the aqueous PEDOT:PSS solution near the μ-tip by varying the dual-plate configuration (μ-tip width, μ-tip length, and shim plate thickness) together with the process variable (i.e., coating speed) and offer design guidelines for the roll-to-roll fabrication of a fine stripe pattern. It can be achieved by reducing the μ-tip length as well as the shim plate thickness and increasing the coating speed until the flow breaks up. This scheme also enables us to raise the stripe density without defects. It is found that the μ-tip length is crucial for coatings of dense stripes. If μ-tip is long, it is not feasible to fabricate dense stripes regardless of the shim plate thickness due to an increase in resistance to flow. It is also found that the wettability of the solution serves as one of the critical parameters that determine the stripe profiles. We have fabricated 100 stripes with the average width of 227 μm and interstripe width nonuniformity as low as 9.2%. Finally, we have fabricated organic light-emitting diodes (OLEDs) atop the conductive PEDOT:PSS stripes and successfully obtained light emission from OLED stripes.**

***Index Terms*— μ-Tips, interstripe width uniformity, organic light-emitting diode (OLED), poly(3,4-ethylenedioxythiophene):poly(4-styrenesulfonate) (PEDOT:PSS) stripes, slot-die coating.**

I. Introduction

SLOT-DIE coating has been widely used to fabricate large-area uniform thin films for various applications including organic electronics for displays and lightings, batteries, organic photovoltaics, and so on [1]–[3]. It provides large-scale roll-to-roll (R2R) production and simultaneous coatings of multiple layers of different solutions [4]–[6]. Recently, there was an attempt to fabricate active-matrix organic light-emitting diode (AMOLED) display panels using two different solution processes, slot-die coating and nozzle printing [7], [8]. Slot-die coating was used for full-area coatings of the common layer [hole injection layer (HIL) or hole transport layer (HTL)], whereas nozzle printing was employed for stripe coatings of the emission layer (EML) (RGB stripes). Such a hybrid process was inevitably used because slot-die coating was not readily available for stripe coatings of pixel arrays. In fact, stripe coating is demanded to fabricate a number of organic devices (unit cells) on a large substrate in one run. The big advantage of stripe coating is that it offers an approach to remove the pixel bank structure used to confine ink droplets in the inkjet printing process [9]–[11]. Homogeneous and continuous stripes can be fabricated by nozzle printing. However, it has a limited process variable (i.e., coating speed) that determines the stripe profiles [12]. Since full-area coatings of the common layers for AMOLEDs are usually performed by a slot coater, a standalone coating system based on slot-die coating would be preferred for all the layers of AMOLEDs. Multiple stripes were fabricated using slot-die coating for organic photovoltaics [13]. Through the numerical simulations of a slot-die head for multiple stripes, T-die and a proper shim were shown to affect the homogeneous flow dynamics [14]. The flow dynamics was also affected by the shim configuration (i.e., slit channel) [15]. In open literature, however, the typical width of stripes fabricated by slot-die coating is of the order of centimeters, which is not applicable to the formation of RGB stripes.

For display applications, highly uniform coatings of multiple stripes as narrow as a pixel width ($\sim$100 μm) and as dense as a pixel array are required. One of the key components of such a coating system is the slot-die head. For coatings of narrow stripes, the slot-die head with the dual plate (shim plate with slit channels and meniscus-guiding plate) is required. In this case, the meniscus is formed between the meniscus-guiding plate and substrate, thereby suppressing capillary widening of stripes. Such a slot-die head with the dual plate was used to fabricate stripe-patterned polymer solar cells [16]. However, it was employed for wide stripes (centimeters in width) that were not suitable for display applications. In this paper, we devise the meniscus-guiding

Manuscript received September 27, 2018; revised November 12, 2018; accepted December 13, 2018. This work was supported by the Ministry of Education through the Basic Science Research Program within the National Research Foundation of Korea (NRF) under Grant NRF-2018R1D1A1B07042248. The review of this paper was arranged by Editor H. Klauk. *(Corresponding author: Jongwoon Park.)*

G. Kim, J. Lee, and D.-K. Shin are with the Interdisciplinary Program in Creative Engineering, Korea University of Technology and Education, Cheonan 330-708, South Korea (e-mail: rlarldmsrns@koreatech.ac.kr; dlwlsdud9203@koreatech.ac.kr; speed21c@koreatech.ac.kr).

J. Park is with the School of Electrical, Electronics and Communication Engineering, Korea University of Technology and Education, Cheonan 330-708, South Korea (e-mail: pjwup@koreatech.ac.kr).

Color versions of one or more of the figures in this paper are available online at http://ieeexplore.ieee.org.

Digital Object Identifier 10.1109/TED.2018.2887213

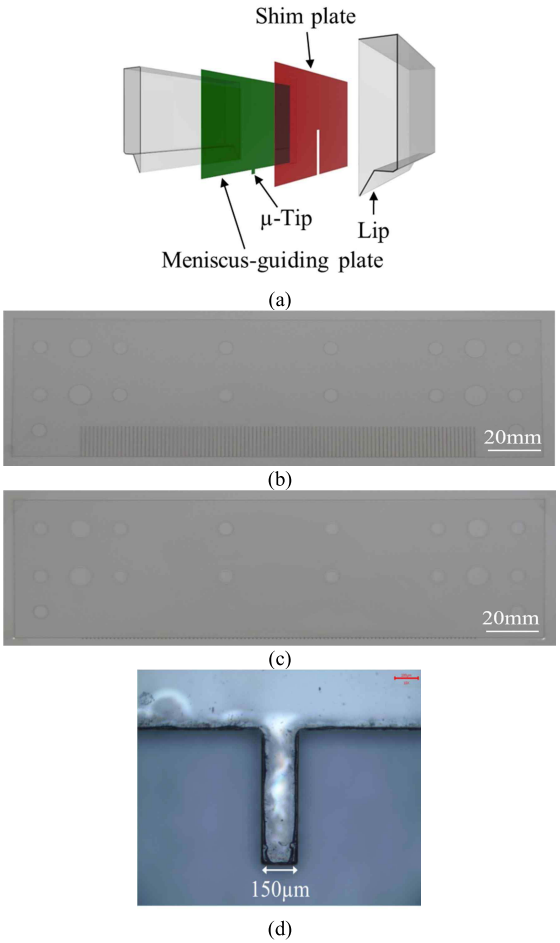

Fig. 1. (a) Schematic view of slot-die head with the dual plate. (b) 100-μm-thick shim plate with a comb pattern. (c) 188-μm-thick meniscus-guiding plate with 100 μ-tips. (d) Magnified image of a 150-μm-wide and 500-μm-long tip in the meniscus-guiding plate.

plate with μ-tip [Fig. 1(a)] for the fabrication of a fine stripe (micrometers in width). Using the slot-die head with meniscus-guiding μ-tip, we have performed R2R stripe coatings of an aqueous organic material and analyzed the flow distribution near the μ-tip, which affects the stripe profiles. To achieve a fine single stripe and dense multiple stripes that are potentially usable in AMOLED displays, we investigate the properties of thin films by varying the dual-plate configuration (μ-tip number, μ-tip width, μ-tip length, and shim plate thickness) together with the process variable (i.e., coating speed). It is demonstrated that highly uniform and dense stripes can be achieved using a thin shim plate and meniscus-guiding plate with narrow and short μ-tips at a relatively high coating speed.

II. Experiment

Multiple stripes, as well as a single stripe, were fabricated using an R2R slot coater that consists of a slot head module (head size: 200 mm × 30 mm × 58 mm, cavity: 156 mm × 2 mm), adjustment range of coating gap between head lip and substrate: 1 μm–35 mm with a resolution of 1 μm, vacuum dry unit (5×10^{-4} Torr), tension and motion controller for the web (web speed: 0.1–100 mm/s), syringe pump system (11 Elite I/W Single, Harvard Apparatus, 0.18 μl/min ∼ 159.8 ml/min), O_3 plasma treatment (0.3 kW), and ionizers. Slot coatings

TABLE I
Summary of Plate Configurations and Process Variables

Parameters	Coating *A*	Coating *B*	Coating *C*	Coating *D*	Coating *E*
Shim plate thickness (μm)	50			25, 50 100	25
Slit width (μm)	150		80, 150 250	150	80
Thickness of meniscus-guiding plate (μm)	-	188			
μ-Tip length (μm)		500			250 500
μ-Tip width (μm)		150	80, 150 250	150	80
Coating speed (mm/s)	20	varied			
Flow rate (ml/min)	0.001				
Coating gap (μm)	20				
Drying	80 °C / 20min				

were carried out on a 170-mm-wide polyethylene terephthalate (PET) film roll, and the effective coating width was 150 mm. The shim and meniscus-guiding plates embedded into the slot head are typically made of a stainless steel material. However, micropatterning of thin (20–100 μm) steel plates requires high-precision processing equipment and thus high manufacturing costs. Instead, we used a cost-effective and easily processable material, PET film, for both plates. The conventional photolithography technique (wet etching) could be applied for micropatterning of the plates. However, it tapered the μ-tip into a point. To avoid it, we employed a laser cutting system (SPD-2000U, EO Technics). Fig. 1(b) and (c) shows the 100-μm-thick shim plate and 188-μm-thick meniscus-guiding plate with 100 μ-tips (150 μm wide and 500 μm long) used for the fabrication of 100 stripes. We can clearly see the flat surface at the end of the μ-tip [Fig. 1(d)], where the meniscus is formed. As an aqueous organic material, poly(3,4-ethylenedioxythiophene):poly (4-styrenesulfonate) (PEDOT:PSS, Clevios AI 4083) was employed, which has been widely used as an HIL of organic light-emitting diodes (OLEDs). As a wetting agent, we added a 0.2 wt% fluorosurfactant into the pristine PEDOT:PSS solution. The viscosity (μ) and surface tension (σ) of the PEDOT:PSS solution are 6 mPa · s and 21.32 mN/m, respectively. Before coating, we used a cellulose acetate disposable syringe filter (0.2 μm, DISMIC-25CS) to filter out aggregated particles existing in the PEDOT:PSS solution. The viscosity and surface tension of solutions were measured using a viscometer (DV-II + Pro viscometer, Brookfield) and tensiometer (sigma702, Biolin Scientific), respectively, at room temperature.

To investigate the coating behaviors of the slot-die head with μ-tip, we fabricated a single stripe by varying the dual-plate configurations (e.g., μ-tip width, μ-tip length, and shim plate thickness) and the process variable (i.e., coating speed). In Table I, we summarized those plate configurations and process variables chosen for the experiments. The coating process was labeled as "Coatings *A*–*E*," depending on the

experiment conditions. With the flow rate (0.001 ml/min) kept unchanged, we varied the coating speed to achieve the narrowest and thinnest stripes. It was increased until the meniscus could not bridge the gap difference between the μ-tip and substrate. We also observed the coating behaviors of the slot-die head with multiple μ-tips by changing the dual-plate configuration (e.g., μ-tip number, μ-tip length, and shim plate thickness). The meniscus near the μ-tip was observed by an area scan camera (acA1300-30gm, BASLER). To capture the μ-tip, substrate, gap clearance, and head lip within one image, we have varied a vertical frame. The actual size can be estimated using scale bars both for horizontal and vertical scales presented in the images. The coated films were predried in the vacuum dry unit for 10 min and hard-baked on a hot plate at 80 °C for 20 min. The film profiles (width and thickness) were measured by 3-D optical surface profiler (NV 6300, ZYGO).

III. Results and Discussion

A. Single Stripe Coatings: Effect of Meniscus-Guiding Plate

We have investigated the effect of the meniscus-guiding plate with μ-tip on slot coatings of a single PEDOT:PSS stripe. To this end, a single stripe was first coated using the slot-die head with the shim plate only under the condition of "Coating *A*" (Table I). To visualize if the coated stripe is straight, we have thermally evaporated 20-nm-thick aluminum (Al) atop the coated stripe and captured the Al-coated side by a camera. Fig. 2(a) shows a long single PEDOT:PSS stripe with the width and thickness of 212 μm and 58 nm, respectively, coated at 20 mm/s. It is observed that the coated stripe is in the form of a zigzag. As illustrated in Fig. 2(b), it is attributed that the meniscus is not pinned stationary during coating. The low-viscosity (6 mPa · s) aqueous solution from the outlet spreads along the gap clearance (i.e., an empty space between the head lip and substrate) and wobbles slightly from side to side during coating. For wide (∼cm) stripe coatings, such a tiny sway is negligible. For narrow (100–200 μm) stripe coatings, especially for display applications, however, it is nonnegligible and regarded as a defect.

Such a tiny but nonnegligible wobble is avoidable using the slot-die head with the dual plate. To demonstrate it, we have coated a single stripe using the 150-μm-wide tip under the condition of "Coating B" in Table I. As apparent in Fig. 2(c) and Table II, the stripe width is controllable by the μ-tip; it is reduced from 212 μm [without the μ-tip at 20 mm/s, Fig. 2(a)] to 166 μm (with the μ-tip at 20 mm/s), which is very close to the μ-tip width. Furthermore, the coated stripe is very straight, as evident in Fig. 2(c). Such positive effects are induced by the μ-tip that can control the flow distribution. Fig. 2(d) exhibits the flow distribution near the μ-tip captured by the area scan camera. In the image, the dashed line represents the PEDOT:PSS solution distributed along the head lip and μ-tip. The dark gray areas (below the dashed lines) indicate the air gap between the head lip and substrate (film). In analogy to the flow distribution in Fig. 2(b), the PEDOT:PSS solution also spreads along the head lip. However, it flows down along the protruded μ-tip, and thus, the meniscus is formed between

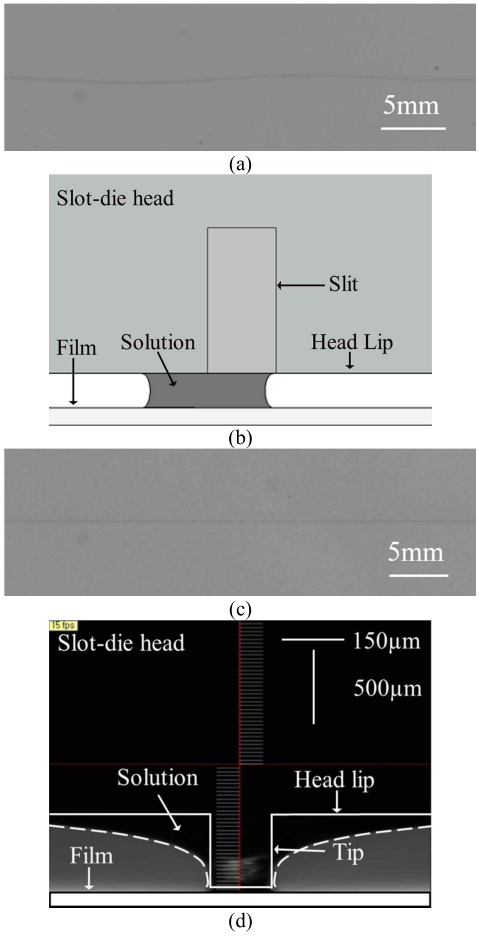

Fig. 2. (a) Long single PEDOT:PSS stripe coated using the shim plate only. (b) Schematic illustration of flow distribution near the slit of the shim. (c) Long single PEDOT:PSS stripe coated using the dual plate with μ-tip. (d) Flow distribution near the μ-tip captured by a vision camera after the meniscus is stabilized.

TABLE II
Measured Width (*W*) and Thickness (*T*) of Stripes Coated With μ-Tips of Different Widths (500-μm-Long Tip and 50-μm-Thick Shim)

	250-μm-wide tip			150-μm-wide tip			80-μm-wide tip		
Velocity (mm/s)	*W* μm	*T* nm	*W*×*T* μm²	*W* μm	*T* nm	*W*×*T* μm²	*W* μm	*T* nm	*W*×*T* μm²
5	357	133	47.5	292	135	39.4	251	161	40.4
7	312	103	32.1	260	122	31.7	213	130	27.7
10	286	88	25.2	243	104	25.3	Line breakup		
20	< tip width	-		166	76	12.6			
25				< tip width	-				

the μ-tip and substrate. Namely, the flow distribution in the absence of the μ-tip is in the shape of rectangle [Fig. 2(b)], whereas it is in the form of inverted triangle in the presence of the μ-tip [Fig. 2(d)]. Since the flow is controlled by the μ-tip, such a tiny sway in the meniscus occurred along the head lip can be suppressed. It is noted that a large amount of fluid is spread along the head lip because the head lip is very hydrophilic to the solution (i.e., the contact angle of the PEDOT:PSS solution on the surface of slot-die head is about 12°) and strong capillary rise occurs along the head lip. We have measured the stripe profiles and presented the results in Fig. 3(a) and Table II. It is apparent that the stripe

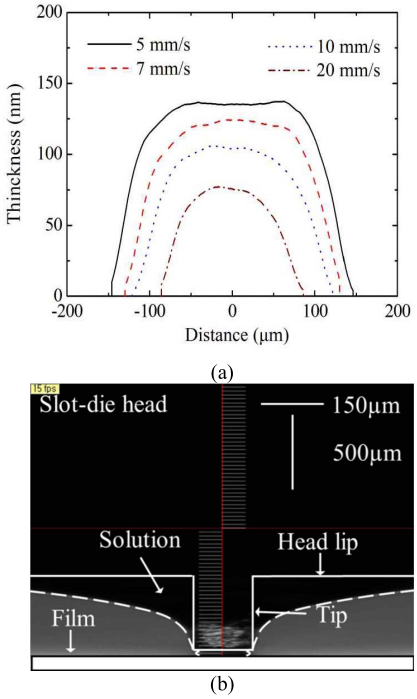

Fig. 3. (a) Measure stripe profiles coated with 150-μm-wide μ-tip for different coating velocities. (b) Image of flow distribution near the μ-tip at the coating speed of 25 mm/s.

width (W) and thickness (T) decrease with increasing coating speed. The W value was calculated as the difference between two points on the x-axis with zero thickness and the T value at the center of the x-axis [at $x = 0$ in Fig. 3(a)]. Since $W \times T$ is inversely proportional to the coating speed, a twofold decrease in the coating speed results in a twofold increase in the $W \times T$ value. It is valid when the coating speed is reduced from 20 to 10 mm/s. However, it is invalid when the coating speed is reduced from 10 to 5 mm/s. As evident in Fig. 3(a), it is attributed that the stripe profile varies depending on the coating speed. No significant change in the stripe profile is observed at high coating speeds (10 and 20 mm/s). However, the stripes become flat and wide near the central region at low coating speeds. Moreover, the stripe thickness at the center is smaller than that at the edges at 5 mm/s, reducing the T value. Otherwise, the T value would increase and the $W \times T$ value would be almost doubled. It is noted that the stripe profile would also vary slightly depending on the ambient humidity during coating and measurement positions. At 20 mm/s, we have obtained a single stripe as thin as 76 nm, which is typical value required for OLEDs. When the coating speed exceeds 20 mm/s, the stripe width becomes narrower than the tip width. As evident in Fig. 3(b), it happens because the dark gray area (i.e., air) appears inward from both edges of the tip end (i.e., the fluid is not spread over the entire tip). It would bring in a tiny wobble in the meniscus and thus unstable stripe coatings.

B. Single Stripe Coatings: Effect of Dual-Plate Configuration

Since the meniscus is formed between the μ-tip and substrate, the stripe width would be affected by the μ-tip width.

TABLE III
MEASURED WIDTH (W) AND THICKNESS (T) OF STRIPES COATED WITH SHIM PLATE OF DIFFERENT THICKNESSES (150-μm-WIDE AND 500-μm-LONG TIP)

	25-μm-thick shim plate			100-μm-thick shim plate		
Velocity (mm/s)	W (μm)	T (nm)	$W \times T$ (μm^2)	W (μm)	T (nm)	$W \times T$ (μm^2)
5	199	67	13.3	-	-	-
7	161	58	9.3	304	173	52.6
10	< tip width	-	-	256	160	40.9
20				204	102	20.8
25				174	83	14.4

To inquire into its effect, we have decreased the μ-tip width from 250 μm down to 80 μm and performed slot coatings under the condition of "Coating *C*." As seen in Table II, the stripe width decreases as the μ-tip width decreases. Meanwhile, the stripe thickness is reduced with increasing μ-tip width because the flow rate is kept unchanged (i.e., the wider the stripe width is, the lower is the stripe thickness). With the 250-μm-wide tip, the stripe width is close to the μ-tip width at 10 mm/s and narrower than the μ-tip width at the coating speeds higher than 10 mm/s. It is due to the fact that the flow rate is fixed, but the slot opening increases by the wide μ-tip (slit width). With the 150-μm-wide tip, the stripe width is close to the μ-tip width at a relatively higher coating speed (20 mm/s) and narrower than the μ-tip width at the coating speeds higher than 20 mm/s. Unexpectedly, however, the 80-μm-wide tip provides the stripe as wide as 213 μm at 7 mm/s. At the coating speeds higher than 7 mm/s, the flow becomes unstable and the meniscus cannot bridge the gap clearance. It is attributed that a small amount of fluid flows through the reduced slot opening (i.e., outlet) and a resistance to flow increases when the μ-tip is long (500 μm). Therefore, the fluid flow along the narrow and long μ-tip becomes more sensitive to the coating speed. We will return to this point later with more experiment results (effect of the μ-tip length).

It is known that the shim plate thickness also determines the slot opening of the die and thus affects the final film thickness. Thin films can be obtained by a thin shim owing to the reduced quantity of fluid from the outlet. To achieve narrower and thinner stripes, therefore, we have reduced the shim plate thickness from 100 μm down to 25 μm and coated under the condition of "Coating *D*." As evident in Table II (50-μm-thick shim and 150-μm-wide tip) and Table III, the stripe width and thickness are reduced with decreasing shim plate thickness at a fixed coating speed (7 mm/s). We can see this behavior from the flow distribution in Fig. 4. As the shim plate thickness is reduced, the quantity of fluid reaching the substrate is reduced and at the same time, the extent to which the fluid spreads along the head lip is suppressed, rendering the stripe narrow. The stripe width becomes close to the μ-tip width at 7 mm/s with the 25-μm-thick shim (Table III), at 20 mm/s with the 50-μm-thick shim (Table II), and at 25 mm/s with the 100-μm-thick shim plate (Table III). Using a thin shim plate, therefore, the coating speed must be

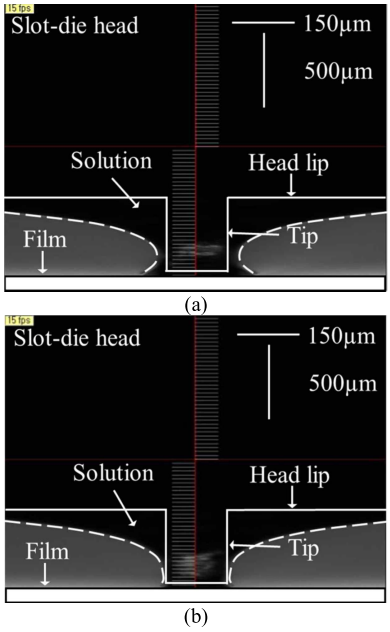

Fig. 4. Images of flow distribution near the 150-μm-wide tip captured by a vision camera at the coating speed of 7 mm/s when the shim plate thickness is (a) 100 μm and (b) 25 μm.

reduced to obtain the same stripe width due to a reduction in the quantity of fluid reaching the substrate.

The μ-tip length would also be crucial because the fluid from the outlet flows along the μ-tip. Its effect has been investigated by reducing the tip length from 500 to 250 μm and performing coatings under the condition of "Coating *E*" (80-μm-wide tip and 25-μm-thick shim). As shown in Fig. 5(a) and (b), the fluid distribution is changed from the inverted triangle shape to the rectangle shape when the μ-tip becomes short. Such a rectangle shape in the fluid distribution in Fig. 5(b) is similar to that formed by the slot-die head with the shim plate only in Fig. 2(b). It is due to the fact that the electronic–hydraulic analogy is observed in the μ-tip. Namely, the μ-tip has some resistance to flow, just as all wires have some resistance to current. If the μ-tip is long, less fluid flows along the tip and accordingly more fluid is distributed along the head lip [Fig. 5(a)]. Conversely, if the μ-tip is short, more fluid flows along the tip and accordingly less fluid is distributed along the head lip [Fig. 5(b)]. When the coating speed is increased from 5 to 12 mm/s, the fluid distribution is recovered to the inverted triangle shape [Fig. 5(c)], enabling the μ-tip to determine the stripe width. As observed earlier, when the μ-tip was long (~500 μm) and the shim plate was thick (~50 μm), the 80-μm-wide tip provided the stripe as wide as 213 μm at 7 mm/s because the flow was unstable at a low coating speed (Table II). When the μ-tip is short (~250 μm) and the shim plate is thin (25 μm), however, the 80-μm-wide tip provides the stripe as narrow as 126 μm. In this case, the flow is stable and the meniscus can bridge the gap clearance even at the coating speed of 12 mm/s (Table IV). To achieve a fine stripe pattern, therefore, it is desirable to utilize a thin shim plate and meniscus-guiding plate with a narrow and short μ-tip and increase the coating speed until just before the flow breaks up.

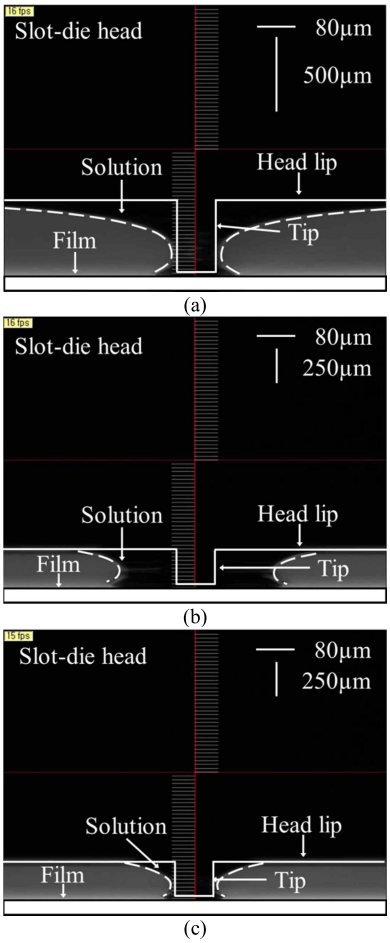

Fig. 5. Images of flow distribution near the 80-μm-wide tip when the μ-tip length and velocity are (a) 500 μm and 5 mm/s, (b) 250 μm and 5 mm/s, and (c) 250 μm and 12 mm/s.

TABLE IV
MEASURED WIDTH (*W*) AND THICKNESS (*T*) OF STRIPES COATED WITH μ-TIPS OF DIFFERENT LENGTHS (80-μm-WIDE TIP AND 25-μm-THICK SHIM)

	500-μm-long tip			250-μm-long tip		
Velocity (mm/s)	*W* (μm)	*T* (nm)	*W*×*T* (μm²)	*W* (μm)	*T* (nm)	*W*×*T* (μm²)
5	210	121	25.4	343	57	19.6
7	Line breakup			187	75	14.0
10				148	67	9.9
12				126	57	7.2

C. Single Stripe Coatings: Effect of Viscosity of PEDOT:PSS

With an attempt to obtain narrower and thinner PEDOT:PSS stripes, we have investigated the effect of the viscosity of the PEDOT:PSS solution. To change its viscosity only, the pristine PEDOT:PSS solution was diluted with deionized water at the mixing ratio of 3:7. Its viscosity was reduced from 6 to 1.8 mPa · s without any change in its surface tension (21.32 mN/m) and contact angle (15.8°) on the substrate. It is evident from Table V that as the viscosity of the PEDOT:PSS solution decreases, the stripe thickness decreases but the stripe width does not change significantly. Namely, the viscosity of the solution, mainly, affects the stripe thickness.

TABLE V
MEASURED WIDTH (W) AND THICKNESS (T) OF STRIPES COATED USING PEDOT:PSS SOLUTIONS WITH DIFFERENT VISCOSITY (150-μm-WIDE AND 500-μm-LONG TIP AND 50-μm-THICK SHIM PLATE)

	Pristine PEDOT:PSS			Diluted PEDOT:PSS		
Velocity (mm/s)	W (μm)	T (nm)	$W\times T$ (μm^2)	W (μm)	T (nm)	$W\times T$ (μm^2)
6	282	127	35.8	285	47	13.4
12	233	97	22.6	225	35	7.9
18	180	78	14	185	27	5

D. Multiple Stripe Coatings

Based on the experiments of a single stripe coating, we have fabricated multiple stripes using the dual plate with multiple μ-tips. In slot-die coatings of wide-width multiple stripes, the width (w) of the stripe for a minimum thickness of the coated layer is given as [17]

$$w = \frac{f_r}{nVH_0}\left[1 + 1.49\left(\frac{\mu V}{\sigma}\right)^{-2/3}\right] \quad (1)$$

where f_r is the flow rate of supplying solution, n is the number of stripes, H_0 is the gap between the slot-head lip and substrate, and V is the coating velocity. When $n = 1$, the required f_r is very low because the target width of the single stripe is as small as 100–200 μm. However, the total f_r must be increased in proportion to n. Therefore, the total flow rate was determined by multiplying the flow rate (0.001 ml/min) fixed for single stripe coatings by the number of stripes (n). Then, we have increased the coating speed (V) until just before the flow at each outlet (μ-tip) breaks up in order to reduce the stripe width further or achieve finer (narrower) stripes. The experiment result is provided only at one coating velocity, beyond which line breakup occurs randomly. To quantify the film quality, we have measured the interstripe width and thickness nonuniformity, defined as [maximum width (thickness) − minimum width (thickness)]/average width (thickness).

Using the dual plate with 150-μm-wide and 500-μm-long tips and 50-μm-thick shim plate, we have first coated 25 stripes at the fixed flow rate of 0.025 ml/min. As summarized in Table VI, the average stripe width and thickness are measured to be 178 μm and 92 nm, respectively. The average width of 25 stripes is wider than the μ-tip width and the single stripe width (166 μm at 20 mm/s). It is because the coating speed cannot be increased higher than 18 mm/s, beyond which line breakup occurs. Such a line breakup is induced by the nonuniform pressure distribution inside the cavity of the slot-die head. It is natural that the uniformity in the pressure distribution along the cavity is degraded as the number of outlets (μ-tips) increases. It will be more serious when the shim plate is thick (i.e., the area of each outlet increases). Consequently, it causes a reduction in the quantity of fluid at some μ-tips and thus line breakup at a lower coating speed. The interstripe width and thickness nonuniformities of 25 stripes are measured to be 11.8% and 8.7%, respectively.

To raise the stripe density, we have increased the number of μ-tips from 25 up to 100 and the flow rate accordingly.

TABLE VI
MEASURED WIDTH, THICKNESS, AND UNIFORMITY OF MULTIPLE STRIPES COATED WITH 150-μm-WIDE TIPS

	25 stripes	50 stripes	100 stripes	
Tip length (μm)	500		250	
Shim thickness (μm)	50		50	25
Coating speed (mm/s)	18		14	
Average width (μm)	178	176	229	227
Average thickness (nm)	92	101	100	103
Inter-stripe width non-uniformity (%)	11.8	13.6	10.4	9.2
Inter-stripe thickness non-uniformity (%)	8.7	12.8	11.9	6.8

We have coated 50 stripes at 18 mm/s and presented the results in Table VI. It is observed that the interstripe width and thickness uniformities are degraded with increasing μ-tip (stripe) number. Using the dual plate with 100 μ-tips, however, it was not feasible to fabricate 100 stripes because the neighboring fluids were merged during coatings. When the stripe density is high, low-viscosity solutions are spread along the head lip and thus fluids from outlets are easily merged [18]. The coating speed was increased to separate them, but some of lines broke up. Such defects (stripe merging and flow breakup) appear because the distance between μ-tips is short, not to mention that the uniformity in the pressure distribution along the cavity is degraded further. The distance between μ-tips in the meniscus-guiding plate with 100 μ-tips is 1.35 mm. As evident in Fig. 2(d), the fluid spreads widely along the head lip and the distance (d_s) from the μ-tip to the point where no fluid exists on the head lip is measured to be about 700 μm. As such, the fluids from the neighboring outlets would merge together on the head lip and flow along the μ-tips without separation. It is evident from Figs. 4 and 5 that d_s can be reduced using a thin shim plate and short μ-tip. Using the 25-μm-thick shim plate and 250-μm-long tip, d_s is reduced down to 100 μm [Fig. 5(c)]. Therefore, the stripe density is expected to be boosted using a thin shim plate and short μ-tips.

To fabricate 100 stripes without defects, we have changed the shim plate thickness and μ-tip length with the μ-tip width (150 μm) kept unchanged. It was not feasible to fabricate 100 stripes when the μ-tip was as long as 500 μm, regardless of the shim plate thickness (25–100 μm). It is attributed that an increase in resistance to flow induced by the long μ-tip causes unstable stripe coatings. With the 250-μm-long tips, we have increased the shim plate thickness up to 100 μm. In this case, fluid merging becomes more severe, especially at those μ-tips located in the middle of the slot-die head. It is due to the fact that the fluid inlet is located in the middle of the cavity and the uniformity in the pressure distribution along the cavity is significantly degraded with increasing slot opening in the presence of 100 μ-tips. With the 250-μm-long tips and the shim plates as thin as 25 and 50 μm, we can fabricate 100 stripes at the coating speed of 14 mm/s, as evident in Fig. 6. Since the coating speed is reduced to 14 mm/s for coatings without defects, the average width of those stripes is increased to 227–229 μm. However, the interstripe

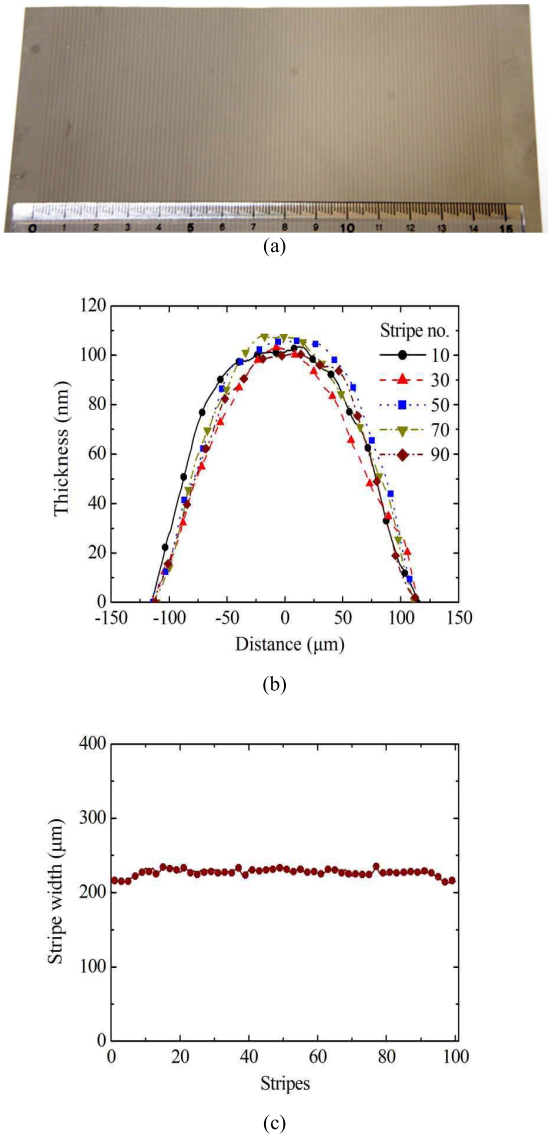

Fig. 6. (a) Image of 100 stripes coated at 14 mm/s using the 25-μm-thick shim plate and meniscus-guiding plate with 150-μm-wide and 250-μm-long tips. (b) Measured stripe profiles for different positions. (c) Measured width of each stripe.

width and thickness uniformities are enhanced. The lowest interstripe width (9.2%) and thickness (6.8%) nonuniformities are achieved using the 250-μm-long μ-tips and 25-μm-thick shim plate (Table VI).

E. Stripe Coatings Using Nonaqueous Solutions

We further investigated the coating behaviors of the aqueous PEDOT:PSS solution by comparison with nonaqueous solutions. To this end, we employed poly(N-vinylcarbazole) (PVK, purchased from Sigma-Aldrich) dissolved in toluene (TE, surface tension = 28.4 mN/m, boiling point (BP) = 110 °C) or ethyl benzoate (EB, surface tension = 35 mN/m, BP = 213 °C, purchased from Sigma-Aldrich). For single stripe coatings, we chose the solute concentration in EB to be 5.0 wt% and flow rate to be 0.0003 ml/min in such a way that the stripe thickness is large enough to be measured. At the same solute concentration, however, the PVK solution with TE distributed along the head lip was easily dried due to its low BP.

TABLE VII
MEASURED WIDTH (W) AND THICKNESS (T) OF SINGLE PVK STRIPE COATED WITH DIFFERENT SOLVENTS (150-μm-WIDE AND 500-μm-LONG TIP AND 50-μm-THICK SHIM PLATE)

	EB (f_r=0.0003 ml/min)				TE (f_r=0.002 ml/min)		
Velocity (mm/s)	W (μm)	T (nm)	$W\times T$ (μm^2)	Velocity (mm/s)	W (μm)	T (nm)	$W\times T$ (μm^2)
5	467	34	15.9	20	353	25	8.8
7	396	25	9.9	30	317	22	7
10	378	22	8.3	40	296	18	5.3
15	246	21	5.2	50	252	14	3.5
-	-	-	-	60	215	12	2.6

To suppress this phenomenon, it was reduced to 1.5 wt% and the flow rate was fixed to be 0.002 ml/min. As summarized in Table VII, the width and thickness of nonaqueous PVK stripes also decrease with increasing coating speed. Compared with the aqueous PEDOT:PSS stripes, however, the PVK stripes with EB or TE are wider and thinner. At the maximum coating speed, the width (246 μm, 215 μm) of the PVK stripe with EB or TE is much greater than the width (166 μm) of the PEDOT:PSS stripe at 20 mm/s (Table II). It seems that the properties of the solution do not significantly affect the stripe profiles because the surface tension (35 mN/m) and viscosity (2.4 mPa · s) of the PVK solution with EB are not much different from those (21.32 mN/m, 6 mPa · s) of the PEDOT:PSS solution. Considering that the stripe width is widened and the stripe thickness becomes smaller with nonaqueous solvents, it is likely to be related to the wettability [i.e., contact angle (θ_c)] of the solution on the substrate. Indeed, θ_c of the PEDOT:PSS solution on the PET film roll was measured to be 15.8°, whereas θ_c of the PVK solution with TE was as low as 11.9° (or unmeasurable) and θ_c of the PVK solution with EB was too low to be measured (<10°). As such, the wettability of the solutions serves as one of the critical parameters that determine the stripe profiles. The contact angle of those solutions would vary depending on the primer material coated on the film rolls.

We also fabricated 100 PVK stripes and presented the images in Fig. 7. To capture a clear image, we added a tiny amount of a red dopant, tris(2-phenylquinoline)iridium(III) (Ir(2-phq)$_3$), into the PVK solutions and shone UV light on the dried samples using a UV hand lamp (VL-4.LC, Vilber Lourmat). Since the PVK solution with EB shows the highest wettability, the PVK stripe with EB has the widest width (average width of 684 μm) at the maximum coating speed of 10 mm/s, followed by the PVK stripe with TE (302 μm at 64 mm/s) and then the PEDOT:PSS stripe (227 μm at 14 mm/s, Table VI).

F. Fabrication of Multiple OLED Stripes

With an attempt to demonstrate the potential applicability of R2R stripe coatings using the slot-die head with μ-tips in AMOLED displays, we have fabricated a single OLED stripe and multiple OLED stripes. In reality, RGB stripe coatings are performed for the EML of AMOLEDs on thin-film transistor backplane where indium-tin-oxide (ITO) is formed for anodes

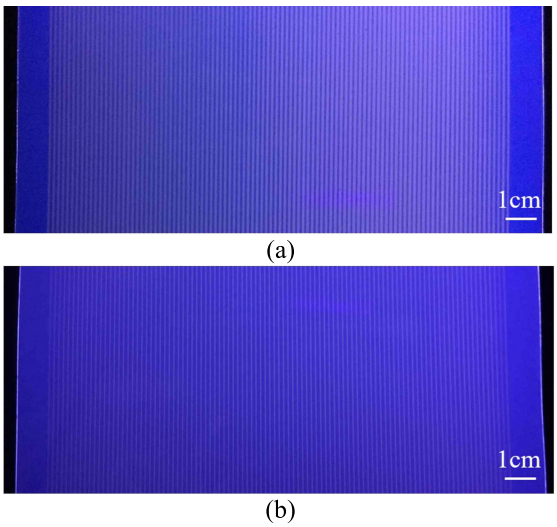

Fig. 7. Image of 100 PVK stripes (a) with EB coated at the maximum coating speed of 10 mm/s and f_r of 0.03 ml/min and (b) with TE coated at 64 mm/s and f_r of 0.2 ml/min using the 25-μm-thick shim plate and meniscus-guiding plate with 150-μm-wide and 250-μm-long tips.

(active pixel areas) [7]. Since pixelated ITO anode on a PET film roll is not readily available, however, we have fabricated multiple PEDOT:PSS (Clevios PH 1000) stripes for anodes on the PET film roll [Fig. 8(a)]. We doped 5 wt% dimethyl sulfoxide to enhance the electrical conductivity of PEDOT:PSS stripes. The conductive PEDOT:PSS stripes fabricated by the dual plate with 100 μ-tips (250-μm-long tips, 25-μm-thick shim plate) under the same coating condition (14 mm/s) show the average width of 250 μm and thickness of 90 nm, which are similar to those PEDOT:PSS (AI 4083) stripes in Table VI. The PEDOT:PSS contact pad was then formed using the conventional slot-die head installed in the R2R slot coater for full-area (coating width of 150 mm) and intermittent coatings. We cut out the PET film on which the conductive PEDOT:PSS stripes and contact pad were formed, attached it to a glass substrate, and loaded it in an organic evaporator to fabricate a phosphorescent green OLED. It consists of 15-nm-thick KHI-001 (Duksan Neolux) for an HIL, 40-nm-thick KHT-001 (Duksan Neolux) for an HTL, 15-nm-thick 4,4'-bis(N-carbazolyl)-1,1'-biphenyl for an EML, 10-nm-thick 4,7-diphenyl-1,10-phenanthroline (Bphen) for a hole/exciton blocking layer, 30-nm-thick LG201(LG Chem., Ltd.) for an electron transport layer, 1-nm-thick lithium fluoride (LiF) for an electron injection layer, and 100-nm-thick aluminum (Al). In the green-emitting layer, 8 wt% fac-tris (2-phenylpyridine)iridium ($Ir(ppy)_3$) was doped. All the layers were deposited sequentially at a rate of 0.5 nm/s under a base pressure of 2×10^{-6} Torr by thermal evaporation. Due to the limited size of vacuum chamber optimized for a 100 mm $\times$ 100 mm substrate, 80 OLED stripes were fabricated on the 100 PEDOT:PSS stripes.

Fig. 8(b) and (c) shows the microscopic electroluminescent photographs from the single OLED stripe and multiple OLED stripes, respectively. Since R2R slot-die coatings were carried out in ambient air (not in a glove box or clean room), the probability of occurrence of a short-circuit phenomenon

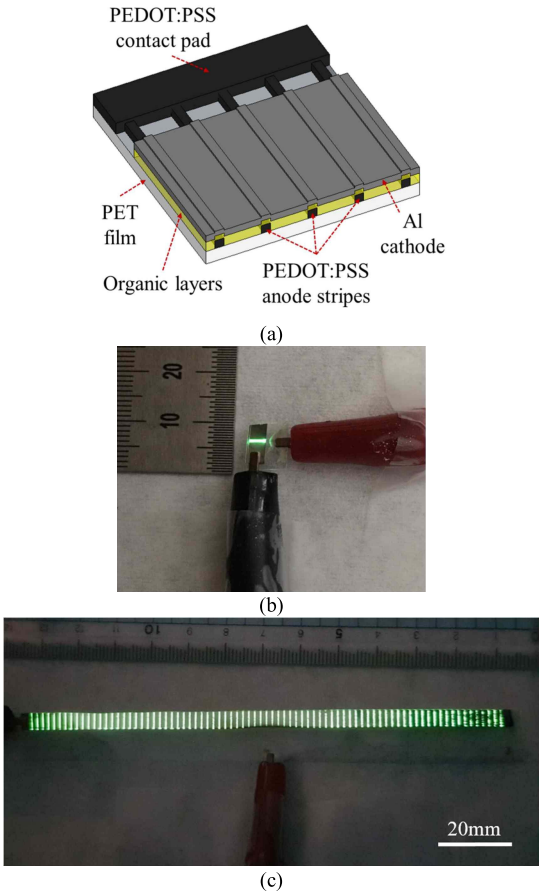

Fig. 8. (a) Schematic view of layer structure for the fabrication of OLED stripes. (b) Image of light emission from single OLED stripe at 7 V. (c) Microscopic electroluminescent photograph from multiple (80) OLED stripes at 5 V.

is high. Even in this situation, we have successfully obtained light emission from those OLED stripes. The width of the light-emitting stripes is observed to be wider than that of the PEDOT:PSS stripes because light emits not only from the top but also from the sides of stripes (i.e., current also flows through the sides of conductive PEDOT:PSS stripes). Meanwhile, the luminance of the OLED stripes located at both ends [Fig. 8(c)] is low. It is because unlike reality, OLED stripes are not controlled individually (i.e., 80 OLED stripes are connected to the single contact pad and thus the current distribution over the stripes is not uniform). Furthermore, dark spots appear in some OLED stripes due to the absence of encapsulation. Even so, this experimental demonstration shows the potential applicability of the proposed coating method to solution-processable AMOLED displays.

IV. Conclusion

We fabricated fine and dense PEDOT:PSS stripes using the slot-die head with protruded μ-tips. In the presence of the μ-tip, the meniscus was pinned stationary, rendering the coated stripes straight. However, the low-viscosity PEDOT:PSS solution was widely spread along the head lip, causing the merging of fluids when μ-tips were located closely. Moreover, the flow broke up easily and randomly during slot coatings

of dense stripes. Such phenomena were suppressed to a great extent using narrow and short μ-tips in combination with a thin shim plate. It is attributed that: 1) the stripe width is determined mainly by the tip width; 2) the uniformity in the pressure distribution along the cavity is enhanced by a thin shim; and 3) a resistance to flow is reduced by a short μ-tip. With this scheme, we fabricated 100 stripes without defects (stripe merging and breakup) and achieved the lowest interstripe width (9.2%) and thickness (6.8%) nonuniformity using the 150-μm-wide tips, 25-μm-thick shim, and 250-μm-long tips. We also addressed that the wettability of the solution could sway the stripe profiles (the higher the wettability is, the thinner and wider the stripe becomes). It is expected that the stripe density can be significantly boosted by optimizing the dual-plate configurations (i.e., further reducing the μ-tip width and length) and deploying two or three slot-die heads without an overlap in the position of μ-tips.

REFERENCES

[1] O. J. Romero, W. J. Suszynski, L. E. Scriven, and M. S. Carvalho, "Low-flow limit in slot coating of dilute solutions of high molecular weight polymer," *J. Non-Newtonian Fluid Mech.*, vol. 118, nos. 2–3, pp. 137–156, Apr. 2004, doi: 10.1016/j.jnnfm.2004.03.004.

[2] M. Schmitt, P. Scharfer, and W. Schabel, "Slot die coating of lithium-ion battery electrodes: Investigations on edge effect issues for stripe and pattern coatings," *J. Coat. Technol. Res.*, vol. 11, no. 1, pp. 57–63, Jan. 2014, doi: 10.1007/s11998-013-9498-y.

[3] O. J. Romero, L. E. Scriven, and M. S. Carvalho, "Slot coating of mildly viscoelastic liquids," *J. Non-Newtonian Fluid Mech.*, vol. 138, nos. 2–3, pp. 63–75, Oct. 2006, doi: 10.1016/j.jnnfm.2005.11.010.

[4] M. S. Carvalho and H. S. Kheshgi, "Low-flow limit in slot coating: Theory and experiments," *AIChE J.*, vol. 46, no. 10, pp. 1907–1917, Oct. 2000, doi: 10.1002/aic.690461003.

[5] C.-F. Lin, D. S. H. Wong, T.-J. Liu, and P.-Y. Wu, "Operating windows of slot die coating: Comparison of theoretical predictions with experimental observations," *Adv. Polym. Technol.*, vol. 29, no. 1, pp. 31–44, Mar. 2010, doi: 10.1889/1.3069746.

[6] B. Park, O. E. Kwon, S. H. Yun, H. G. Jeon, and Y. H. Huh, "Organic semiconducting layers fabricated by self-metered slot-die coating for solution-processable organic light-emitting devices," *J. Mater. Chem. C*, vol. 2, no. 40, pp. 8614–8621, 2014, doi: 10.1039/C4TC00817K.

[7] R. Chesterfield, A. Johnson, C. Lang, M. Stainer, and J. Ziebarth, "Solution-coating technology for AMOLED displays," *Inf. Display*, vol. 27, no. 1, pp. 24–30, Jan. 2011.

[8] T. J. Faircloth, J. G. Innocenzo, and C. D. Lang, "Slot die coating for OLED displays," in *SID Symp. Dig. Tech. Papers*, vol. 39, no. 1, pp. 645–647, Jul. 2012, doi: 10.1889/1.3069746.

[9] H. Liu *et al.*, "Line printing solution-processable small molecules with uniform surface profile via ink-jet printer," *J. Colloid Interface Sci.*, vol. 465, pp. 11–106, Mar. 2016, doi: 10.1016/j.jcis.2015.11.067.

[10] M. Singh, H. M. Haverinen, P. Dhagat, and G. E. Jabbour, "Inkjet printing-process and its applications," *Adv. Mater.*, vol. 22, no. 6, pp. 673–685, 2010, doi: 10.1002/adma.200901141.

[11] D. Soltman and V. Subramanian, "Inkjet-printed line morphologies and temperature control of the coffee ring effect," *Langmuir*, vol. 24, no. 5, pp. 2224–2231, Jan. 2008, doi: 10.1021/la7026847.

[12] D. G. Yoon, M.-G. Kang, J. B. Kim, and K.-T. Kang, "Nozzle printed-PEDOT: PSS for organic light emitting diodes with various dilution rates of ethanol," *Appl. Sci.*, vol. 8, no. 2, pp. 203–207, Jan. 2018, doi: 10.3390/app8020203.

[13] R. Søndergaard, M. Hösel, D. Angmo, T. T. Larsen-Olsen, and F. C. Krebs, "Roll-to-roll fabrication of polymer solar cells," *Mater. Today*, vol. 15, nos. 1–2, pp. 36–49, 2012, doi: 10.1016/S1369-7021(12)70019-6.

[14] S.-H. Wen and T.-J. Liu, "Extrusion die design for multiple stripes," *Polym. Eng. Sci.*, vol. 35, no. 9, pp. 759–767, May 1995, doi: 10.1002/pen.760350905.

[15] G. H. Han, S. H. Lee, W.-G. Ahn, J. Nam, and H. W. Jung, "Effect of shim configuration on flow dynamics and operability windows in stripe slot coating process," *J. Coat. Technol. Res.*, vol. 11, no. 1, pp. 19–29, Jan. 2014, doi: 10.1007/s11998-013-9485-3.

[16] F. C. Krebs, "Fabrication and processing of polymer solar cells: A review of printing and coating techniques," *Sol. Energy Mater. Sol. Cells*, vol. 93, no. 4, pp. 394–412, Apr. 2009, doi: 10.1016/j.solmat.2008.10.004.

[17] H. Kang, J. Park, and K. Shin, "Statistical analysis for the manufacturing of multi-strip patterns by roll-to-roll single slot-die systems," *Robot. Comput.-Integr. Manuf.*, vol. 30, no. 4, pp. 363–368, 2014, doi: 10.1016/j.rcim.2013.12.004.

[18] S. M. Raupp *et al.*, "Slot die stripe coating of low viscous fluids," *J. Coat. Technol. Res.*, vol. 15, no. 5, pp. 899–911, Sep. 2018, doi: 10.1007/s11998-017-0039.

Authors' photographs and biographies not available at the time of publication.